MPPT Enabled Solar Photo Voltaic Generators with V-f and P-Q Control in Micro grids

E.v.kishore[1], C. Ashok kumar[2], M. Venkata kishore[3]
Balaji Institute of Technology & Sciences, Lingapuram, Andhra Pradesh, India.

***Abstract*: The micro grid concept allows small distributed energy resources (DERs) to act in a coordinated manner to provide a necessary amount of active power and ancillary service when re- quire. This paper proposes an approach of coordinated and integrated control of solar PV generators with the maximum power point tracking (MPPT) control and battery storage control to pro- vide voltage and frequency (V-f) support to an islanded micro grid. Also, active and non active/reactive power (P-Q) control with solar PV, MPPT and battery storage is proposed for the grid connected mode. The control strategies show effective coordination between inverter V-f (or P-Q) control, MPPT control, and energy storage charging and discharging control. The paper also shows an effective coordination among participating micro resources while considering the case of changing irradiance and battery state of charge (SOC) constraint. The simulation studies are carried out with the IEEE 13-bus feeder test system in grid connected and islanded micro grid modes. The results clearly verify the effectiveness of pro- posed control methods. The simulations are carried out in Mat lab and Simpowersystems.**

***Keywords*: Active and reactive power control, distributed energy resource (DER), distributed generation (DG), maximum power point tracking (MPPT), voltage and frequency control, solar photovoltaic (PV).**

1. Introduction

The micro grid is a collection of distributed generators or micro resources, energy storage devices, and loads which operate as a single and independent controllable system capable of providing both power and heat to the area of service The micro resources that are incorporated in a micro grid are comprised of small units, less than 100 kW, provided with power electronics (PE) interface. Most common resources are Solar Photovoltaic (PV), Fuel Cell (FC), or micro turbines connected at the distribution voltage level.

In a micro grid, the micro sources and storage devices are connected to the feeders through the micro source controllers (MCs) and the coordination among the micro sources is carried out by the central controller (CC) .The micro grid is connected to the medium voltage level utility grid at the point of common coupling (PCC) through the circuit breakers. When a micro grid is connected to the grid, the operational control of voltage and frequency is done entirely by the grid; however, a micro grid still supplies the critical loads at PCC, thus, acting as a PQ bus. In islanded condition, a micro grid has to operate on its own, independent of the grid, to control the voltage and frequency of the micro grid and hence, acts like a PV (power-voltage) bus. The operation and management in both the modes is controlled and coordinated with the help of micro source controllers (MCs) at the local level and central controller (CCs) at the global level. Similar to the traditional synchronous generator frequency control the micro grid voltage and frequency control can also be performed using droop control methods .

The present work provides fast response characteristics for voltage and frequency control as compared to the secondary control considered. The analogy between inverter control and the synchronous generator control in an islanded micro grid is studied in detail in [9]. In the islanded mode, there is the necessity of having a reference voltage and frequency signals in the micro grid inverter control. The operation and control of the inverter interface of renewable-based distributed energy resources (DERs), like Solar Photovoltaic (PV) in a micro grid, is a real challenge, especially when it comes to maintaining both micro grid voltage and frequency within an acceptable range. A voltage control method based on traditional droop control for voltage sag mitigation along with voltage ride through capability is proposed.

A dynamic voltage regulation based on adaptive control is proposed in However, there are not many research works performed on V-f or P-Q control using solar PV including MPPT control and battery storage in micro grids. In frequency regulation with PV in micro grids is studied; however, this work does not consider the voltage control objective and lacks battery storage in the micro grid. In a small scale PV is considered in a grid-connected mode to control the active and reactive power of the system. Here, the control methods consider abc-dq0 transformation and vice versa which is avoided in the present paper. In power modulation of solar PV generators with an electric double layer capacitor as energy storage is considered for frequency control. In load frequency control is implemented in micro grid with PV and storage; however, this work also lacks the consideration of a voltage control objective. The voltage and frequency control with solar PV and battery in micro grid with an induction machine is investigated in however, this work does not ex- plain the transfer mechanism of controls to consider the battery SOC constraint.

In summary, the previous works in this topic either lack the incorporation of an energy storage component or the voltage control objective along with frequency control or the incorporation of control transition in different scenarios. The present work full's these gaps by considering all of these objectives. This paper proposes several control algorithms through which the capability of PV generators for voltage and frequency (V-f) control and active and nonnative/reactive power (P-Q) control in islanded and grid connected micro grids could be harnessed. Detailed models of PV, battery, inverter and converter are considered for the study.

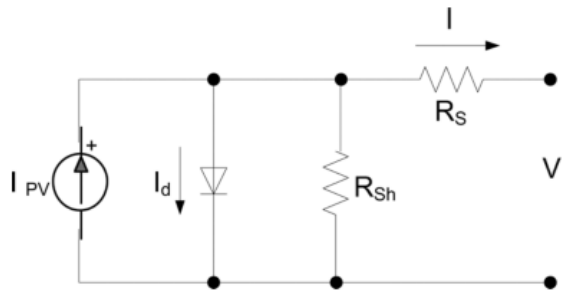

Fig. 1. One diode equivalent circuit of Solar PV.

The major contribution and novelty of the proposed control methods lie in the coordination among individual proposed control methods: MPPT control at the PV side, battery control, and V-f/P-Q control algorithm at the inverter side. These three control algorithms at three stages are jointly linked through a power balance objective at the DC and AC side of the inverter so that the DC side voltage is indirectly controlled at the desired value in order to maintain the AC side voltage at the utility desired voltage. Also, the proposed control methods have the capability of handling battery state of charge (SOC) constraints through the coordination of controls between participating micro resources in the micro grid. This is a very important contribution from this work as compared to other literatures in this area. At the same time, the controls can seamlessly transform from one mode e.g., inverter P-Q control in grid connected mode to V-f control in islanded mode. The proposed control methods are validated with satisfactory results. The controls are developed in abs reference frames using the RMS/average values of voltages and active and reactive power. Hence, it is easy and efficient to implement, and avoids the transformation to and from other reference frames which greatly simplexes the control strategies. The chosen control parameters in the proposed methodologies are, however, dependent on the PV, battery, and external power grid conditions. These parameters can be adaptively achieved with the changing system conditions which could be a very promising future direction of this work. The rest of the paper is organized as briery presents the analytical modeling of Solar PV with model validation results. Shows the PV system configuration, describes the modeling of the battery storage, and pro- vides information about the structure distribution feeder under study. Section V describes the proposed coordinated V-f and P-Q control algorithms while incorporating PV MPPT control and battery storage control. Section VI presents convincing results to prove the effectiveness of the proposed control algorithms. Finally, summarizes the major contributions of the paper.

2. Solar PV Modeling and Validation

The commonly accepted solar cell model is a one diode model , This work uses the single diode model of the solar cell to model the Kyocera KC200GT solar array,

$$I = I_{\mathrm{PV}} - I_0 \left[\exp\left(\frac{V + R_s I}{V_{\mathrm{therm}} a} \right) - 1 \right] - \frac{V + R_s I}{R_{\mathrm{sh}}} \quad (1)$$

which is shown, where and are the photo current and the diode saturation currents, respectively; is the thermal voltage of the array, being the cells connected in series for greater output voltage, is the Boltzmann constant (Kelvin) is the temperature of

the p-n junction of the diode, and (C) is the electron charge; and are the equivalent series and shunt resistances of the array, respectively,

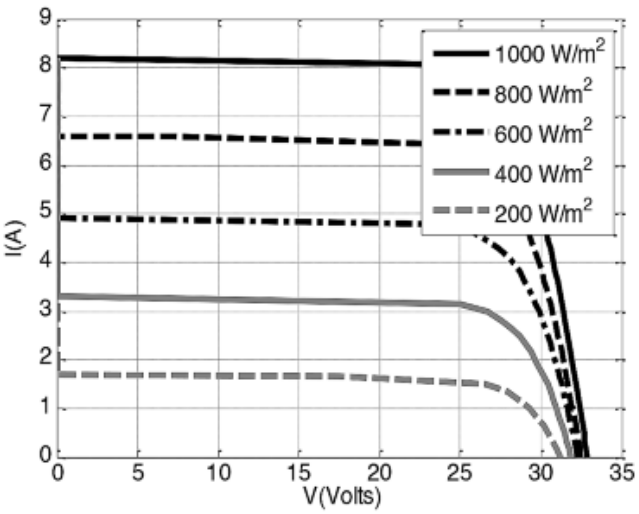

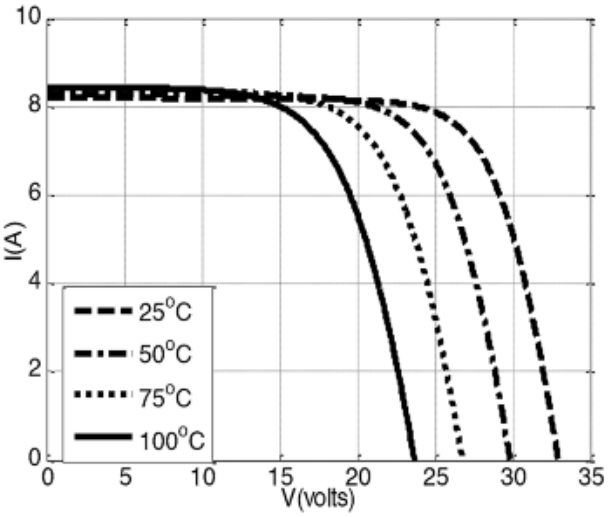

Fig. 2: varying irradiance at a cell temperature of 25 C

Fig .3: varying cell temperature at 1000W/m .

factor usually chosen in the range . Here is taken as 1.The photocurrent of the PV array depends linearly on

TABLE I

PV PANEL PARAMETERS AT 1000 W/M^2 AND 25°C

Model	Kyocera KC200GT
P_{MPP}	200W
V_{MPP}	26.30V
I_{MPP}	7.61A
V_{OC}	32.90V
I_{SC}	8.21A

$$I_{\mathrm{PV}} = (I_{\mathrm{PV},n} + K_1 \Delta T)\frac{G}{G_n}$$

- (2)

where is the photocurrent at the standard test condition (sty, 25 c and 1000 w/m is the short circuit current/ temperature coefficient; is the difference between the actual and nominal temperature in Kelvin; is the irradiation on the device surface; and is the nominal radiation, both in w/m .

$$I_{\mathrm{PV},n} = \frac{R_{\mathrm{sh}} + R_s}{R_{\mathrm{sh}}} I_{\mathrm{sc}}$$

- (3)

using these fundamental equations and parameters from the data sheet, the pv model is developed and varied with the panel datasheet. the i-v characteristics of kc200gt for different irradiance levels at the cell temperature of 25 c and varying cell temperature for a constant irradiance level of 1000 w/m as obtained from the simulation are shown in figs. 2(a) and (b), respectively. the similarities of the i-v curves for different conditions with the corresponding curves in the kc200gt panel datasheet prove the validity of the developed solar panel model. the parameters of the pv panel under study are shown in table.

The PV system under study for the proposed V-f and P-Q control has 125 strings with each string having 4 series connected panels. The Maximum Power Point (MPP) for a single panel of KC200GT at 1000 W/m and 25 C (STC) is 200 W. Hence, the maximum power of the PV generator at STC is

3. PV System Configuration and System Description:

(A) PV System Configuration

fig. 3 shows the pv system configuration for v-f and p-q control with pv operating at mpp including the battery storage backup. it is a two-stage configuration where a dc-dc boost converter is used for mppt control. the system also considers a battery back-up in case of emergencies while maintaining the voltage and frequency of the micro grid or while trying to supply the critical loads**.** A battery is connected in parallel to the pv to inject or absorb active power through a bidirectional dc-dc converter. When the battery is absorbing power, the converter operates in the buck mode and when battery is injecting power to the grid, it operates in the boost mode. The operation mode is maintained through the control signal provided to the converter switches. The pv system is connected to the grid through a coupling inductor . the coupling inductor alters out the ripples in the pv output current. the connection point is called the point of common coupling (pcc) and the pcc voltage is denoted as . the rest of the system in fig. 3 denotes the idée 13-bus distribution feeder which is implied as a substation with the feeder equivalent impedance, . the details of the ieee-13 bus system will be described in the next section. the pv source is connected to the dc link of the inverter with a capacitor . the pv is the active power source.

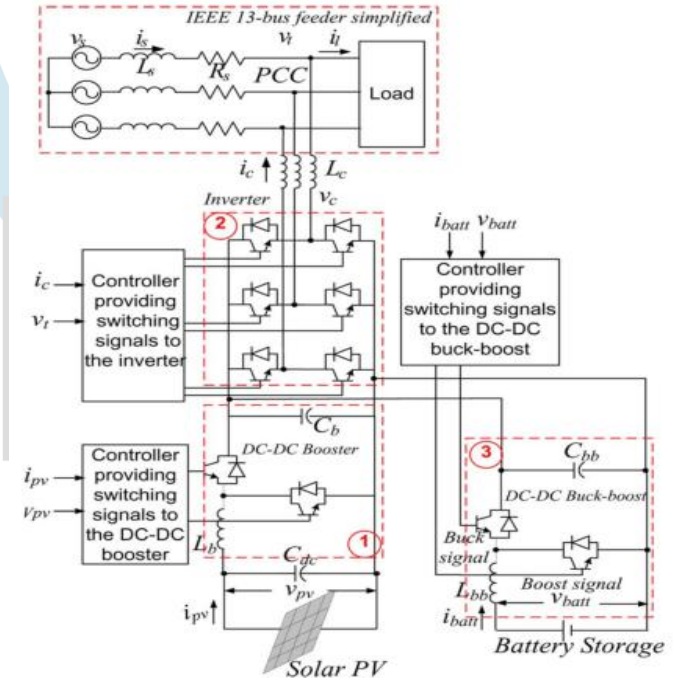

Fig . 4: System configuration of V-f control with solar PV generator operating at MPPT with a battery storage system.

neglected, respectively, then the average power of the PV de- noted as , the apparent power and the average reactive power of the PV are as given below.

$$S(t) = V_t(t)I_c(t) = \frac{v_t(t)}{\omega L_c}\sqrt{V_t(t)^2 + V_c(t)^2 - 2V_t(t)V_c(t)\cos\alpha}$$

$$P(t) = \frac{2}{T}\int_{t-\frac{T}{2}}^{t} v_t(\tau)i_c(\tau)d\tau = \frac{V_t(t)V_c(t)}{\omega L_c}\sin\alpha$$

$$Q(t) = \sqrt{S^2(t) - P^2(t)} = \frac{V_t(t)}{\omega L_c}(V_c(t)\cos\alpha - V_t(t))$$

- (4)

Here, is the phase angle of relative to the PCC voltage. and in (4) and (6) can be approximated by the firstterms of the Taylor series if the angle is small.

$$P(t) \approx \frac{V_t(t)V_c(t)}{\omega L_c}\alpha$$
$$Q(t) \approx \frac{V_t(t)}{\omega L_c}(V_t(t) - V_c(t))$$

- (5)

(B) Battery Modeling:

In this paper, the battery model is taken from the MATLAB SimPowerSystems library with appropriate parameters which will be used for the proposed V-f and P-Q controls. The detailed description about the battery model is given in Due to the intermittent and uncertain nature of solar power output and also the highly punctuating load demands, deep cycle lead acid batteries are the most common type of battery storage in micro- grid applications because the maximum capacity of the battery can be utilized.

Hence, in this paper, a battery is modeled as a lead acid battery with appropriate choice of parameters for deep cycle application. It is assumed that the lead acid battery can be discharged up to SOC of 20% and can be charged up to SOC of 80%.

$$V_{\text{Batt}} = V_0 - R\cdot i - K\frac{Q}{Q-\text{it}}(\text{it} + t^*) + \text{Exp}(t)$$
$$V_{\text{Batt}} = V_0 - R\cdot i - \left[K\frac{Q}{\text{it} - 0.1Q}\right]i^* - \left[K\frac{Q}{Q-\text{it}}\right] + \text{Exp}(t)$$

- (6)

where is the battery voltage (v), is the battery constant voltage (v), is polarization constant (v/ah) or polarization resistance is battery capacity (ah),battery charge (ah), is exponential zone amplitude (v),is exponential zone time constant inverse (ah), is the internal resistance is battery current (a), and is filtered current (a).

backup power to compensate for the pv generation in the case of a very small or no irradiance level. in this work, the mpp of pv generator at stc is 100 kw. hence, the battery is chosen to provide this amount of power for a maximum of 1 hour with an energy content of 100 kwh. the battery backup is consid- ered for short duration applications like frequency control and supplying power to critical loads in the event of emergency sit- uations. one hour of battery backup is considered to be enough for other backup generators to take over the controls in the mi- crogrid emergency situations.

(C) Description of 13-bus distribution feeder:

the diagram of the ieee 13-bus distribution test system is shown in fig. 4. it consists of a substation, 13 buses or nodes, 11 line sections, and 8 loads. the loads comprise of a combi- nation of constant impedance, constant current, and constant power (zip) loads but most of them are constant power loads. the substation is at 115 kv and it is stepped down to 4.16 kv by a distribution transformer (t1). there is one more transformer (t2) which steps down 4.16 kv to 480 v.

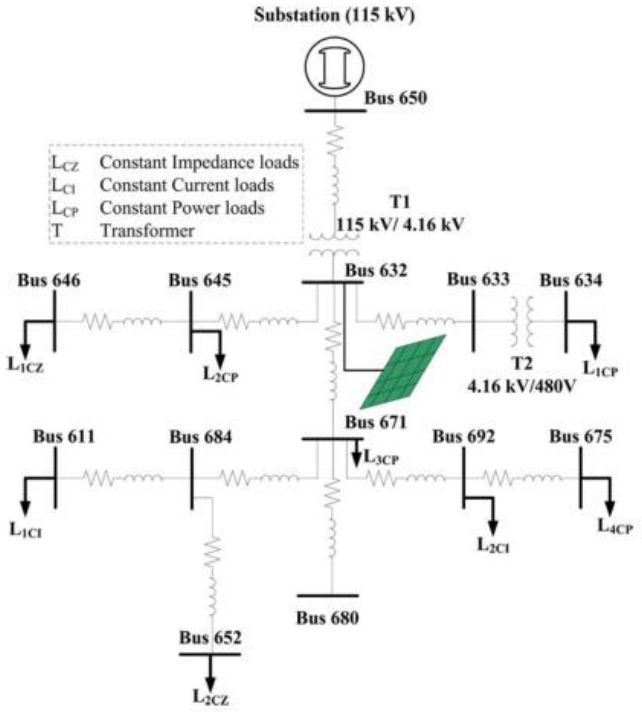

Fig: 5 ieee-13 bus distribution feeder.

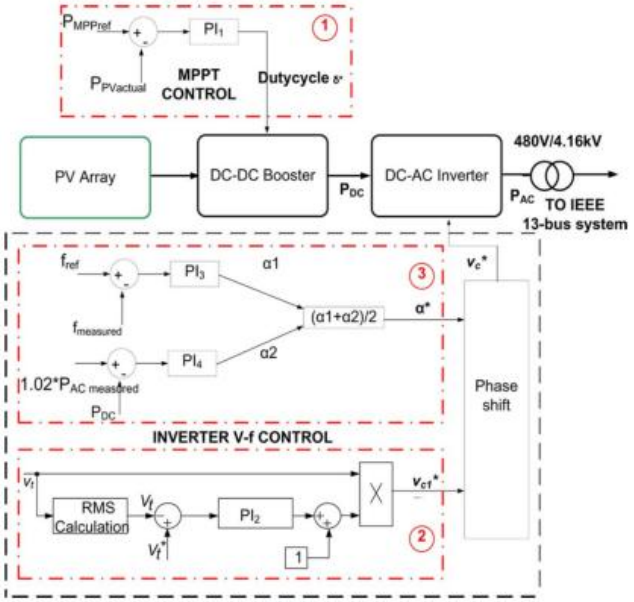

Fig: 6 integrated solar pv mppt and v-f control diagram.

4. MPPT AND BATTERY INTEGRATED V-F AND P-Q CONTROL:

the mppt and battery integrated v-f control diagrams are shown in figs. 5 and 6, respectively. the control comprises of one loop for mppt control, two different loops for v-f control at the inverter side and another loop for battery power management.

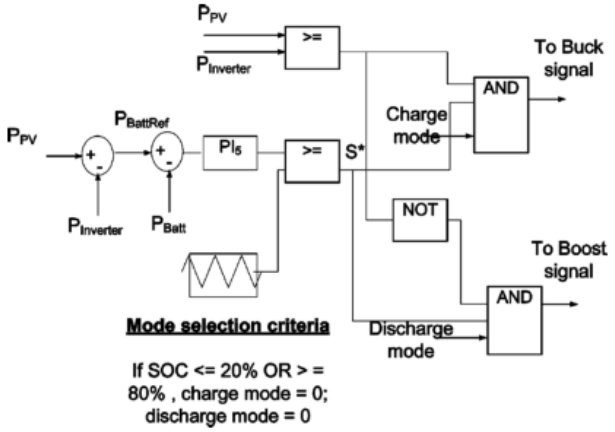

Fig 7: battery power control diagram.

us mpp. then, it compares the actual pv power output, with this reference and feeds this error to a pi controller, which outputs the duty cycle for the dc-dc booster so that the array always operates at the referenced point. the equation for this control loop is given by (11). here, and are the controller proportional and integral gains respectively

$$v_{c1}^{*}(t) = v_t(t)\left[1 + K_{P2}(V_t^{*}(t) - V_t(t)) + K_{I2}\int_0^t ((V_t^{*}(t) - V_t(t))dt)\right] \quad \delta^{*} = K_{p1} * (P_{\mathrm{MPPref}} - P_{\mathrm{PV}}) + K_{i1} * \int_0^t (P_{\mathrm{MPPref}} - P_{\mathrm{PV}})dt.$$

$$\alpha_1^{*} = K_{P3}(f_{\mathrm{ref}} - f_{\mathrm{measured}}) + K_{I3}\int_0^t (f_{\mathrm{ref}} - f_{\mathrm{measured}})dt$$

- (7)

there is another controller used in the same loop 3. this controller maintains active power balance between the ac and dc sides of the inverter. the reference signal for is obtained from the dynamically changing active power injection from the inverter at the ac side as determined by the output of . the measured ac side active power, is multiplied by a factor of 1.02 considering the efficiency of inverter as 98% such that the dc side active power is 102% of the ac side active power. the dc side active power is compared with this value of ac side power and the error is fed to to obtain the phase shift contribution from this loop as . the equation for this control.

$$\alpha_2^{*} = K_{P4}(1.02 * P_{\mathrm{AC}} - P_{\mathrm{DC}}) + K_{I4}\int_0^t (1.02 * P_{\mathrm{AC}} - P_{\mathrm{DC}})dt.$$

$$S^{*} = K_{P5}(P_{\mathrm{Battref}} - P_{\mathrm{Batt}}) + K_{15}\int_0^t (P_{\mathrm{Battref}} - P_{\mathrm{Batt}})dt.$$

- (8)

when there is abundant solar irradiance available and the active power required for the microgrid frequency control is less than active power produced by the pv generator at mpp i.e., and at the same time the battery soc is 80%, then, the battery cannot be charged beyond this upper limit of soc. in such case, decreasing the output power of pv generator would lead to underutilization of the solar re- source. hence, a global control mechanism is required in a mi- crogrid which can transition the pv control from frequency control mode to constant power mode with power to be generated at . meanwhile, there should be a mechanism to allow any other generator of the micro grid to handle the frequency control problem. in the micro grid system under consideration, there is a diesel generator which can decrease its generation in order to match the pv generation increase. hence, the power balance of the system will be maintained in order to control the microgrid frequency.

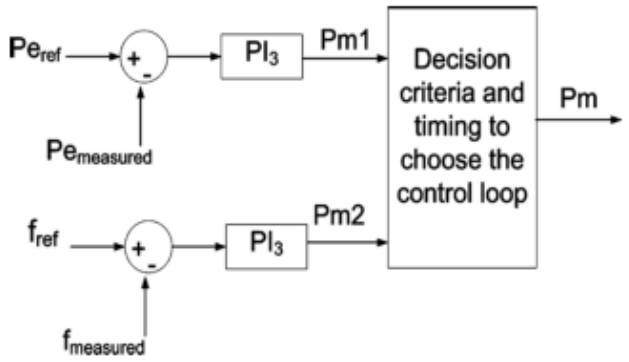

Fig. 8. diesel generator control transition.

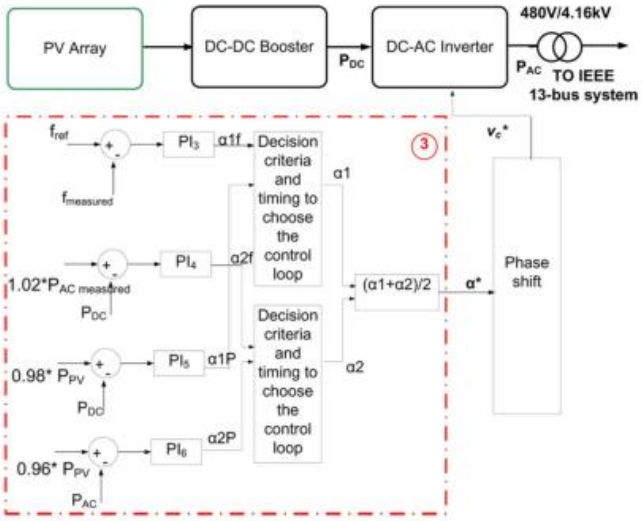

Fig :9: modification of pv inverter frequency control loop.

and the measured electrical power to generate the mechanical power reference, the frequency error is considered in the con- trols. fig. 8 shows the modification in frequency control loop of the pv inverter which includes the transition to another constant active power control loop. during the simulation process, the transition time is heuristically selected as 8 sec so that the smoothness in the transfer of controls can be observed.

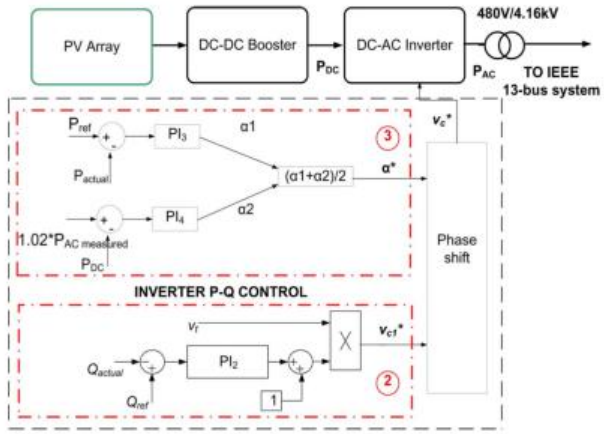

fig. 9. integrated solar pv mppt and pq control diagram.

control strategy is applicable particularly for such cases. the mppt control part for generating the duty cycle of a proper control for the dc-dc boost converter is the same as described in section v-a above and hence, will not be explained here. thus, fig. 9 shows the p-q control blocks only, leaving behind the mppt control block which is also present in the entire integrated control system. the p-q control initially proposed in [22] and implemented in a larger system in [23] is converted to a more robust control with the integration of mppt control and battery storage control in the present work.

the inverter side p-q control is slightly modified version of inverter v-f control. it is entirely based on the relationship of ac- tive and reactive power at pcc with inverter output phase and voltage magnitude as given by the (7) and (8), respectively. in

fig. 9 (loop 2), the measured reactive power injection at pcc is compared with the referenced reactive load and this error signal is passed to the pi controller, . then, the term ob- tained is multiplied by the terminal voltage to obtain the ref- erence voltage which is in phase with . the control loop 3 in fig. 9 handles active power control through the controller, to generate the phase shift contribution and at the sametime insure the active power balance between ac and dc sides through the controller, . this is already explained in detail in section v-a for v-f control. thus, the equations for p-q control

$$
\begin{aligned}
v_{c1}^{*} &= (K_{P2}(Q_{\text{ref}} - Q_{\text{actual}}) \\
&\quad + K_{I2}\int_{0}^{t}(Q_{\text{ref}} - Q_{\text{actual}})dt + 1)v_t \\
\alpha_1^{*} &= K_{P3}(P_{\text{ref}} - P_{\text{actual}}) \\
&\quad + K_{I3}\int_{0}^{t}(P_{\text{ref}} - P_{\text{actual}})dt \\
\alpha_2^{*} &= K_{P4}(1.02 * P_{\text{ACmeasured}} - P_{\text{DC}}) \\
&\quad + K_{14}\int_{0}^{t}(1.02 * P_{\text{ACmeasured}} - P_{\text{DC}})dt \\
\alpha^{*} &= (\alpha_1^{*} + \alpha_2^{*})/2
\end{aligned}
$$

- (10)

equation represents the reactive power control loop, represents the active power control loop, and ensures the active power balance between the dc and ac sides of the inverter. equation averages the phase shift contribution obtained from the active power control at the ac and dc sides

TABLE II
CONTROLLER GAIN PARAMETERS FOR V-F CONTROL (CASE 1)

MPPT Control Loop	K_{p1}	6×10^{-8}
	K_{i1}	6×10^{-6}
Voltage Control Loop	K_{p2}	0.0004
	K_{i2}	0.005
Frequency Control Loop	K_{p3}	9.9×10^{-4}
	K_{i3}	5×10^{-3}
P_{DC} Control Loop	K_{p4}	0.8×10^{-9}
	K_{i4}	0.8×10^{-8}
Battery Control Loop	K_{p5}	1.5×10^{-8}
	K_{i5}	1.5×10^{-7}

5. Simulation results:

(A) test of v-f control in microgrid mode:

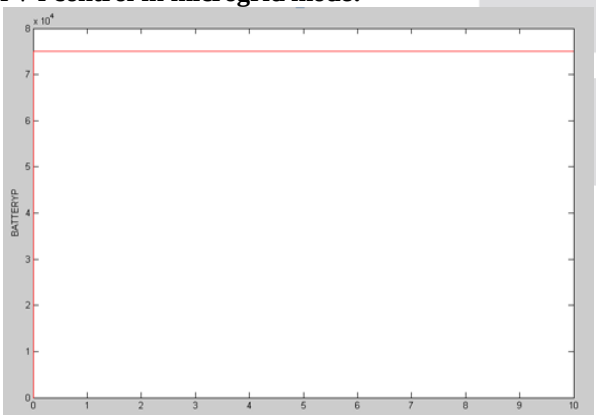

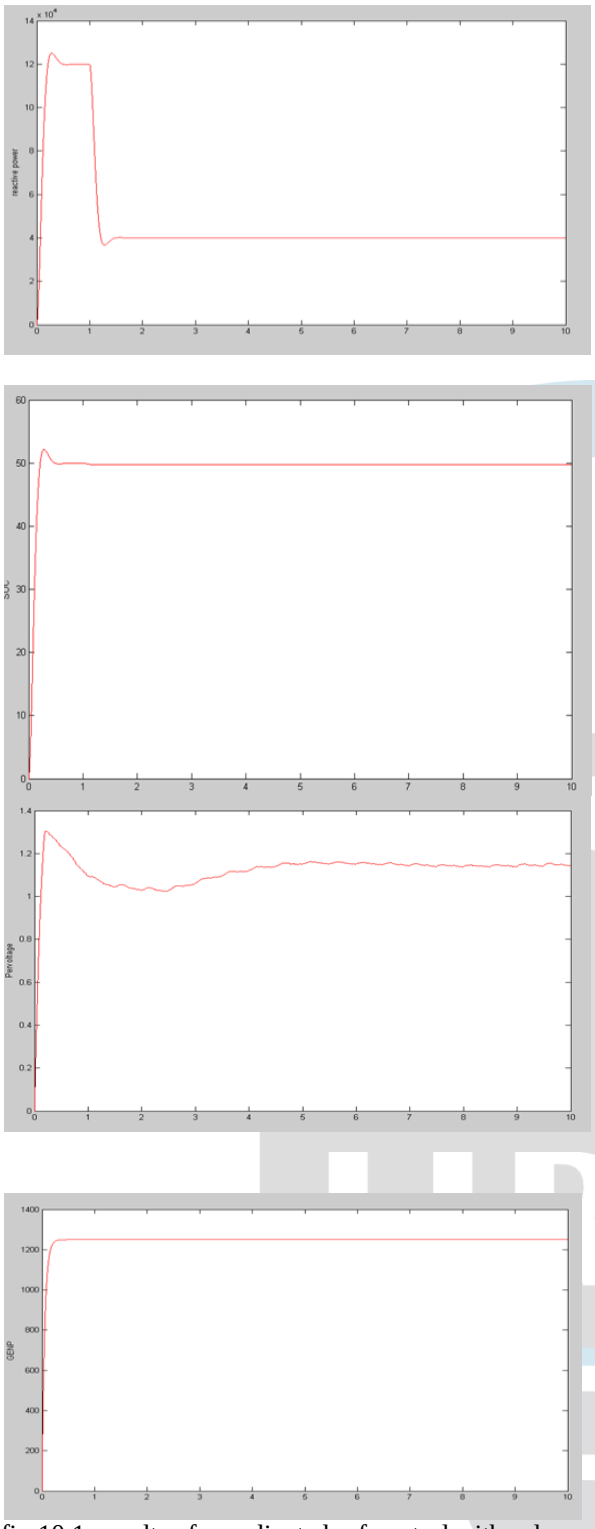

fig:10.1 results of coordinated v-f control with solar pv including mppt control and battery control**.**

(b) test of v-f control showing transition from grid connected to islanded microgrid mode:

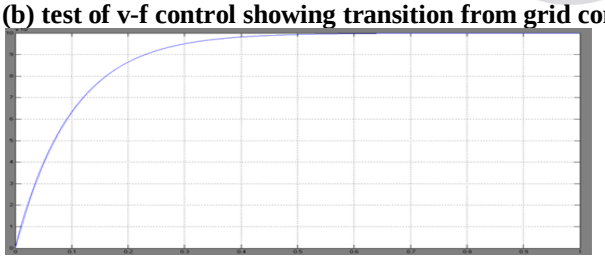

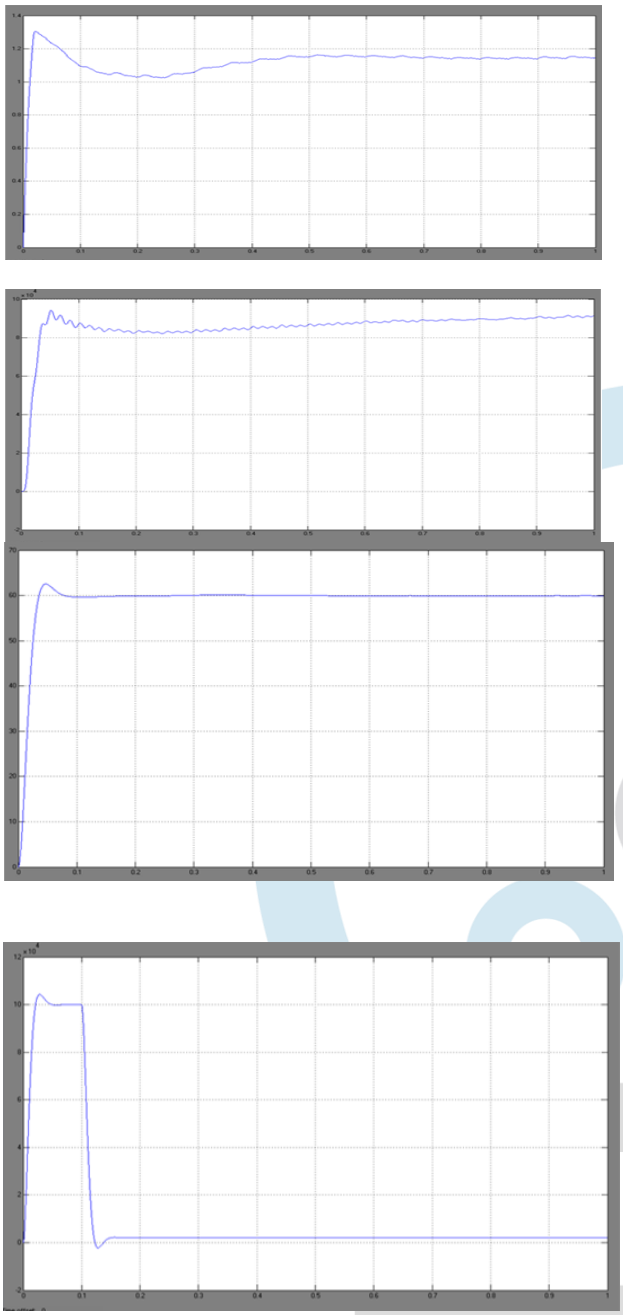

Fig: 10.2: . results of v-f control showing grid to microgrid transition.

CONCLUSION

In this dissertation, first, the application of PhV-based DER systems for active and nonactive power control is investigated with a simulation study of the IEEE 13 bus distribution test system. The dynamic response of the PhV in following the local load pattern is presented. The ability of the DERs to provide nonactive (reactive) power in addition to active (real) power is very beneficial in maintaining the voltage stability and power flow control in future power systems.

A method of MPPT control and PCC voltage control is developed. An indirect control of DC side voltage by maintaining the balance in power transfer at every stage from PhV to inverter output is proposed and investigated. Next, a voltage and frequency control algorithm for microgrid applications using solar PhV operating at MPPT along with BESS is proposed. The capability of PhV in controlling both voltage and frequency of microgrid can provide a greater incentive to the increased penetration and deployment of sustainable PhV generation in future microgrids. Again, the method of MPPT control and BESS control is also integrated with the proposed P-Q control algorithm so as to supply the critical loads of the microgrids in the event of emergency. The results presented clearly prove the effectiveness of this control technique.

REFERENCES

[1] R. H. Lasseter, "MicroGrids," in Proc. IEEE Power Engineering Society Winter Meeting, 2002, vol. 1, pp. 305–308.

[2] S. Chowdhury, S. P. Chowdhury, and P. Crossley, "Microgrids and ActiveDistribution Networks," 2009, IET Renewable Energy Series 6.

[3] H. Saadat, Power System Analysis, 2nd ed. New York, NY, USA:Mc-Graw Hill, 2002.

[4] J. A. P. Lopes, C. L. Moreira, and A. G. Madureira, "Defining control strategies for MicroGrids islanded operation," IEEE Trans. Power Syst., vol. 21, pp. 916–924, 2006.

[5] B. Awad, J.Wu, and N. Jenkins, "Control of distributed generation," Electrotechn. Info. (2008), vol. 125/12, pp. 409–414.

[6] J. C. Vasquez, J. M. Guerrero, E. Gregorio, P. Rodriguez, R. Teodorescu, and F. Blaabjerg, "Adaptive droop control applied to distributed generation inverters connected to the grid," in Proc. 2008 IEEE ISIE, pp. 2420–2425.

[7] H. Bevrani and S. Shokoohi, "An intelligent droop control for simultaneous voltage and frequency regulation in islanded microgrids," IEEE Trans. Smart Grid, vol. 4, no. 3, pp. 1505–1513, Sep. 2013.

[8] J. C. Vasquez, J. M. Guerrero, M. Savaghebi, and R. Teodorescu, "Modelling, analysis and design of stationary reference frame droop controlled parallel three-phase voltage source inverters," in Proc. 2011 IEEE 8th ICPE & ECCE, pp. 272–279.

[9] T. L. Vandoorn, B. Meersman, J. D. M. De Kooning, and L. Vandevelde, "Analogy between conventional grid contro and islanded microgrid control based on a global DC-link voltage droop," *IEEE Trans. Power Delivery*, vol. 27, no. 3, pp. 1405–1414, Jul. 2012.